*Geofísica Internacional (2005), Vol. 44, Num. 1, pp. 103-111*

# Subsidence of the Laguna Salada Basin, northeastern Baja California, Mexico, inferred from Milankovitch climatic changes

Juan Contreras[1], Arturo Martín-Barajas[1] and Juan Carlos Herguera[3]
[1] *Departamento de Geología, CICESE, Ensenada Baja California, México*
[2] *División de Oceanología, CICESE, Ensenada Baja California, México*

Received: July 2, 2003; accepted: April 27, 2004

**RESUMEN**

La cuenca de Laguna Salada en el norte de Baja California, México, es un semigraben activo producto de la tectónica transtensional del Golfo de California. Esta cuenca endorréica es sensible a cambios en sedimentación por variaciones en el aporte de sedimentos de fuentes cercanas y distales transportados por arroyos de las sierras adyacentes y por el Río Colorado. Esta cuenca es un sitio excepcional para explorar el uso de cambios climáticos cíclicos como herramienta de datación y estimar tasas de sedimentación y subsidencia en el área. Para demostrar esto se presenta un análisis de series de tiempo de un registro de rayos de gama de un pozo geotérmico exploratorio perforado adyacente a la falla de Laguna Salada, la cual limita el margen oriental de la cuenca. Los resultados del análisis indican que el espectro de los primeros 980 m del registro de rayos gama tiene una alta coherencia con el espectro de registros isotópicos paleoclimáticos de $\delta^{18}O$ del Pleistoceno, los cuales exhiben fuerte periodicidad de Milankovitch. Con base en esto, es posible correlacionar estadios climáticos con paquetes sedimentarios cortados por el pozo. De esta manera es posible constreñir las edades de los sedimentos depositados durante los últimos 780 kiloaños con una incertidumbre estimada en 10 ka. También se deriva un modelo sencillo de conversión de profundidad a tiempo para la cuenca de Laguna Salada. El modelo indica que la tasa de sedimentación para los últimos 780 ka ha permanecido constante con un valor de ~1.6 mm/año. Dada la proximidad del sito de perforación a la falla de Laguna Salada, tomamos este valor como la tasa de subsidencia de esta falla.

**PALABRAS CLAVE:** Periodicidad de Milankovitch, provincia transtensional del Golfo de California.

**ABSTRACT**

Laguna Salada in northern Baja California, Mexico, is an active half-graben product of the trans-tensional tectonics of the Gulf of California. It is sensitive to changes in sediment supply from the Colorado River basin. We present a time series analysis of the upper 980 m of a gamma-ray log from a borehole drilled near the Laguna Salada fault. The power spectrum of the gamma-ray log resembles the spectrum of $\delta^{18}O$ Pleistocene isotopic variations from ice cores and from the deep ocean, known to be strongly controlled by Milankovitch cycles. We correlate $\delta^{18}O$ stages with silty and sandy intervals in the log. Downcore ages for the last 780 ky are constrained within ~10 kyr. We derive a simple time vs. depth calibration relation for the basin over this time interval. Estimated sedimentation rates at the drill site appear to be constant with a value of ~1.6 mm/yr. We propose that this subsidence rate is produced by the Laguna Salada fault.

**KEY WORDS:** Gulf of California extensional province, Milankovitch cyclicity.

## INTRODUCTION

The Laguna Salada Basin (LSB) is a rift basin in Baja California, Mexico (Figure 1a), located between Sierra de Juárez and Sierra de Cucapá, and to the south of the Salton Trough. It lies on the North America-Pacific plate boundary and is an active asymmetric graben with major subsidence along its eastern margin, *i.e.,* the Laguna Salada-Cañada David Fault system (Savage *et al.*, 1994; García-Abdeslem *et al.*, 2001; Dorsey and Martín Barajas, 1999; Martín-Barajas *et al.*, 2001). Sedimentation in Laguna Salada began during the Pleistocene when uplift of Sierra Cucapá, a 700 m-high block of crystalline basement, cut off this region from the Colorado River delta plain and the Salton Trough to the NE (Figure 1b and c). This new structural configuration favored the formation of a semi-closed depocenter with an inlet at its southern part connecting the basin with the delta plain and tidal flats of the northern Gulf of California, which allows for the occasional inflow of runoff from the Colorado River (Figure 1b).

Although presently Laguna Salada is a barren lakebed, in historical times and up to 1936 coinciding with the filling of the Hoover Dam- it was a shallow lacustrine environment year round fed by waters originating from the annual spring snowmelts and rains in the Colorado Plateau and the Rocky Mountains. Sediments in the basin, therefore, are composed of fine grained sediments transported by the Colorado River interfingered with coarse grained alluvial and delta fan deposits derived from local sources along Sierra Juárez and

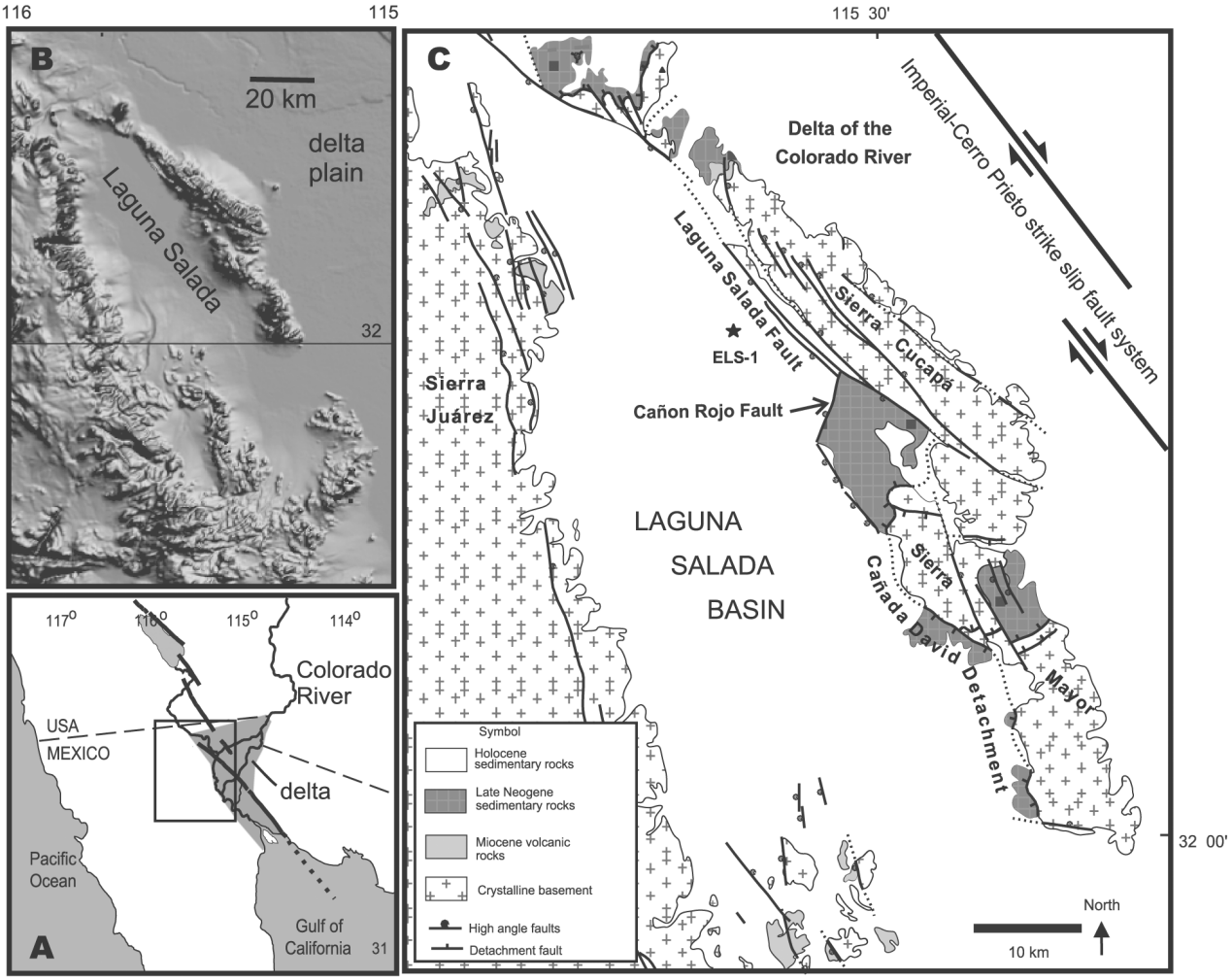


Fig. 1. (A) Map of western North America showing the location of the Laguna Salada basin. (B) Digital elevation model of the Laguna Salada basin. (C) Simplified geologic map of the Laguna Salada region showing the main structures in the area. Star indicates the location of the ELS1 geothermal exploratory well (after Martín-Barajas *et al.*, 2001).

Sierra Cucapá (Figure 1b and c). Analysis of sediments from three exploratory wells drilled by the Mexican Power Company (CFE) indicates that a 980 m-thick succession of sand and silt was deposited under these lacustrine conditions (Martin-Barajas *et al.*, 2001). This contrasts with deeper and coarser sediments in the basin with a more convoluted origin likely related to the early tectonic activity of the Laguna Salada fault and the workings of the ancient delta of the Colorado River (Martín Barajas *et al.*, 2001).

Precise determinations of rates of sedimentation, subsidence, and extension in the LSB, as for most rift basins of the northern Gulf of California, are fraught with large uncertainties due to lack of reliable dating (*e.g.*, Axen and Fletcher, 1999; Axen *et al.*, 2000; Muller and Rockwell, 1994) or due to very long baselines of geodetic measurements (Savage *et al.*, 1994). Here we explore the use of the response of sedimentation to cyclic climatic changes as a chronological tool, to constrain long-term sedimentation and tectonic subsidence rates of this complex part of the North America-Pacific plate boundary. The morphological characteristics of Laguna Salada enhances the sensitivity of this basin to changes in sediment supply, and set it apart as a unique place to investigate the response of sedimentation to Milankovitch cyclicity. Sedimentary variability in other rift basins is modulated by precession, obliquity, and eccentricity cycles displaying a hierarchical stratigraphic arrangement with well-defined thickness ratios, like the 1:5 precession to eccentricity relation (Olsen and Kent, 1998; and references therein).

To find out if the stratigraphy of the LSB is indeed modulated by Milankovitch climatic changes we carried out

a time series analysis of the upper 980 m of a gamma-ray log from the ELS1 borehole, one of the exploratory geothermal wells drilled by CFE (Figure 1c) and contrasted it with climatic proxies for the last 1 Ma. Our goal is to establish how much of the variability observed in the wire line log can be attributed to such changes. Natural emission of gamma-ray particles correlates inversely with grain size and we interpret its fluctuation downcore as an indirect proxy for past changes in the production of sediments derived from distal and local sources, e.g., alternations of clayey and silty levels (maxima in gamma-ray emission) deposited by the Colorado River with the sands and gravels from local sources (minima in gamma-ray emission).

## METHODOLOGY

The employed methodology is that of time series analysis, which focuses on finding deterministic (periodic) and non-deterministic (stochastic) behavior in discrete and continuous series. A basic description of the employed methodology is presented in Appendix A. We only present a general description of the procedures and results description of the employed computer algorithms can be found in numerous textbooks of numerical analysis (e.g. Press *et al*., 1992).

The first step in our analysis was to detrend the upper 980 m of the gamma-ray log then, we calculate the discrete autocorrelation function of the square of the residual to document the log's fundamental frequencies. We take the square of the residuals to amplify maxima and minima, thus enhancing repetitive sedimentary patterns contained in the log. We then compare the spectra of the residual with Pleistocene variations of $\delta^{18}O$ from ice and deep-sea records and establish a visual correlation between the gamma-ray signal from ELS1 and the time calibrated $\delta^{18}O$ climatic records to construct a high resolution Quaternary time scale for the LSB. This chronological framework is then used to derive the sedimentation and subsidence rates at the ELS1 drilling site.

## RESULTS

Statistically significant peaks appear at lag distances of 14, 18, 28, 36, and 130 m in the discrete autocorrelation function of the square of the residual of the gamma-ray log ($\lambda_1$ through $\lambda_4/2$ in Figure 2a). This indicates the residual of the signal is composed of repetitive patterns spaced by these distances. A similar conclusion can be drawn from the power spectrum of the gamma-ray log shown in Figure 2b: the signal is not random; its decomposition in sinusoidal waveforms indicates energy is concentrated at specific frequencies. Moreover, these frequencies have approximately the same wavelengths as the ones obtained from autocorrelation ($\lambda_1$ through $\lambda_3/2$ in Figure 2a). However, the power spectrum shows the existence of an additional fundamental frequency of 0.015 cycle/m (~66 m). We interpret these frequencies as responses of sedimentation to climatic forcing induced by Milankovitch orbital changes, *i.e*., the 142-130 m sedimentary cycles are associated with 95 kyr eccentricity cycles, 66 m cycles with 41 kyr obliquity cycles, 36 m cycles with 23 kyr precession cycles, 28 m cycles with 19 kyr precession cycles, and the 16-14 m cycles are sub-harmonics of the 23 kyr and 19 kyr precession cycles, respectively. Table 1 presents a comparison of the ratios of the wavelengths (thickness) from the spectrum and the lag distances from the autocorrelation diagram with the ratios of Milankovitch cycles. The ratios of the ELS1 log are in good agreement with the ratios predicted by orbital theory, supporting our idea that climatic forcing controls cyclicity in this basin.

We also carried out a cross-spectral analysis between ELS1 log and $\delta^{18}O$ signal from the Vostok ice cores in Antarctica (Petit *et al*., 1999). Variations of $\delta^{18}O$ isotopic ratios in these ice cores correlate with warming and cooling at high latitudes and we use them to further assess the control of low frequency climatic changes on sedimentation in the LSB. In Figure 2c we converted the Laguna Salada spectrum to the time domain using a sedimentation rate of 1.5 mm/yr, obtained from the correspondence of the 36 m cycle to the 23 kyr Milankovitch cycle, centering both spectra at the 0.045 $kyr^{-1}$ frequency. The cross-spectral comparison shows that both spectra have similar energy distributions, especially in the frequency range 0.025-0.09 $kyr^{-1}$. The energy content departs significantly in the low frequency range; the Vostok data shows a larger concentration of power at the 100 kyr wavelength than the detrended gamma-ray log. Coherence between gamma ray and $\delta^{18}O$ data is significantly high at the main orbital bands (>0.95) and decrease to 0.5-0.8 in the frequency bands between them. The strong resemblance between the spectra suggests, once again, that sedimentation in LSB is controlled by climatic changes related to the contraction and expansion of ice sheets at high latitudes.

Two long climatic records were chosen to further constrain ages of sedimentary horizons in the ELS1 gamma-ray log by means of a visual correlation: the time-calibrated $\delta^{18}O$ signal from the Vostok ice cores (Petit *et al*., 1999), which is used to date the upper part of the log, and the deep-sea benthic $\delta^{18}O$ record from site ODP 677 (Shackleton *et al*., 1990), which is used to date the lower part of the gamma ray log. Although the signal from ODP 677 covers the entire log we decided to use the Vostok time series because of its higher resolution and its remarkable similarity with the ELS1 wire line log. However, observe that our correlation starts at oxygen isotope stage 5 (130 ka before present) because the upper 150 m of the gamma-ray log were not recorded by CFE (Figure 3).

To correlate climatic and sedimentation events between the ELS1 and Vostok signals we aligned maxima associated with the 100 kyr eccentricity cycle (solid lines in Figure 3).

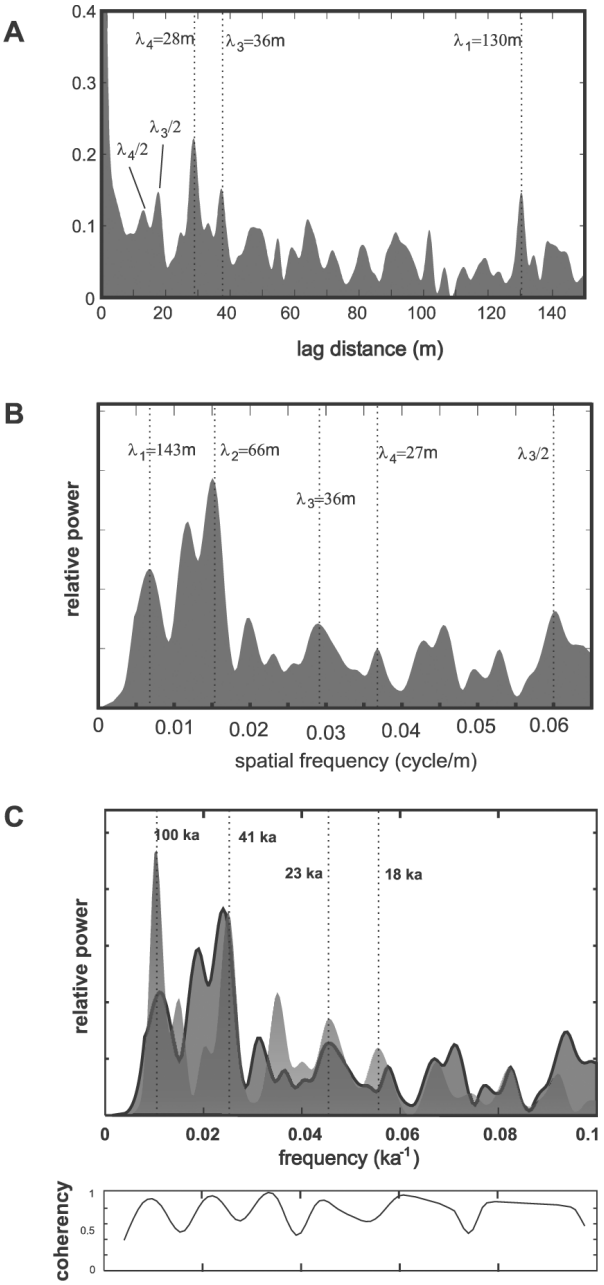


Fig. 2. (A) Discrete autocorrelation function of the uppermost 980 m of ELS1 gamma-ray log in Laguna Salada basin for lag distances of up to 200 m (see Figure 1 for location of the drill site). (B) Spectrum of the log in space domain. (C) Cross-spectral analysis between the spectrum of ELS1 gamma-ray log converted to time domain (solid line) and the spectrum of the $\delta^{18}O$ from Vostok ice core. The graph at bottom shows the coherence between signals.

Then, we matched interestadial features associated with precession and obliquity cycles (dashed lines in Figure 3). The similarity between the $\delta^{18}O$ and the gamma-ray log (Figure 3a) is remarkably high given the fact these signals are recording different attributes. This is especially true for the first two eccentricity cycles, which have cross-correlation values as high as 0.85 and 0.80 (Figure 3a).

Minima were matched for ODP 677 benthic isotopic data because they are more clearly expressed; interestadial features were not considered given the lower resolution of ODP 677 data. The lowermost 400 m of the log also show a good similarity with the benthic foraminifera $\delta^{18}O$ data from OPD 677 site (Figure 3b). Oxygen isotope stages 12 and 13 appear anomalously thick in the gamma-ray log and are rather subtle. In contrast, stages 15 through 19 have a good expression in the log, though stages 16 and 17 are considerably thinner than expected.

## DISCUSSION

### Climatic and sedimentological implications

The signals contrasted in this article are of different nature and their correlation should not be taken as a comparison of two climatic records, *i.e.,* warm (maxima) periods in the $\delta^{18}O$ data do not necessarily coincide with warm periods in LSB. It also must be observed that in carrying our correlation we decided to align the 100 kyr maxima because the uppermost 150 m of the log are missing. Although this may look arbitrary, the rationale behind this alignment rests on the assumption that during odd warm climatic stages the higher sea-level at the mouth of the Gulf allows for the diversion of part of the Colorado River discharge into the LSB, and the deposit of its fine grained bedload on the bed of this basin, as it was the case until the construction of the Hoover Dam in the decade of 1930. During cold stages the drop in sea level (up to 120 m below the current sea level) at the upper Gulf forces a seaward progradation of the Colorado delta and the coastline by tens of km to the south. The ensuing encroachment of the river to its lower base level isolates LSB from the Colorado rivershed and favors the filling by local sources from the nearby Sierras through alluvial fans channeling a coarser and less classified sediment load onto the lakebed.

### Sources of uncertainties in the correlation and construction of a depth vs. time model for the Laguna Salada basin

Our age determinations contain several sources of uncertainty related to the different tuning models of the oxygen isotopic curves (for ODP 677 site see Imbrie and Imbrie, 1980; Shackleton *et al.*, 1993; for the Vostok ice cores see Petit *et al.*, 1999), locations in different hemispheres, and resolutions. Perhaps the former is the largest source given ages of isotopic maxima of interglacial periods differ by as much as one half of a precession cycle. For example, in the

**Table 1**

Comparison of the ratios of the thickness of cycles in Laguna Salada basin and ratios of Milancovitch cycles

| **Ratios** | $\lambda_1/\lambda_2$ | $\lambda_1/\lambda_3$ | $\lambda_1/\lambda_4$ | $\lambda_3/\lambda_4$ |
|---|---|---|---|---|
| Autocorrelation | - | 3.61 | 4.64 | 1.28 |
| Power spectrum | 2.1 | 3.97 | 5.07 | 1.28 |
| Milancovitch* | 2.43 | 4.1 | 5.00 | 1.21 |

* values for these cycles are $\lambda_1$=95 kyr, $\lambda_2$=41 kyr, $\lambda_3$=23 kyr, and $\lambda_4$=19 kyr.

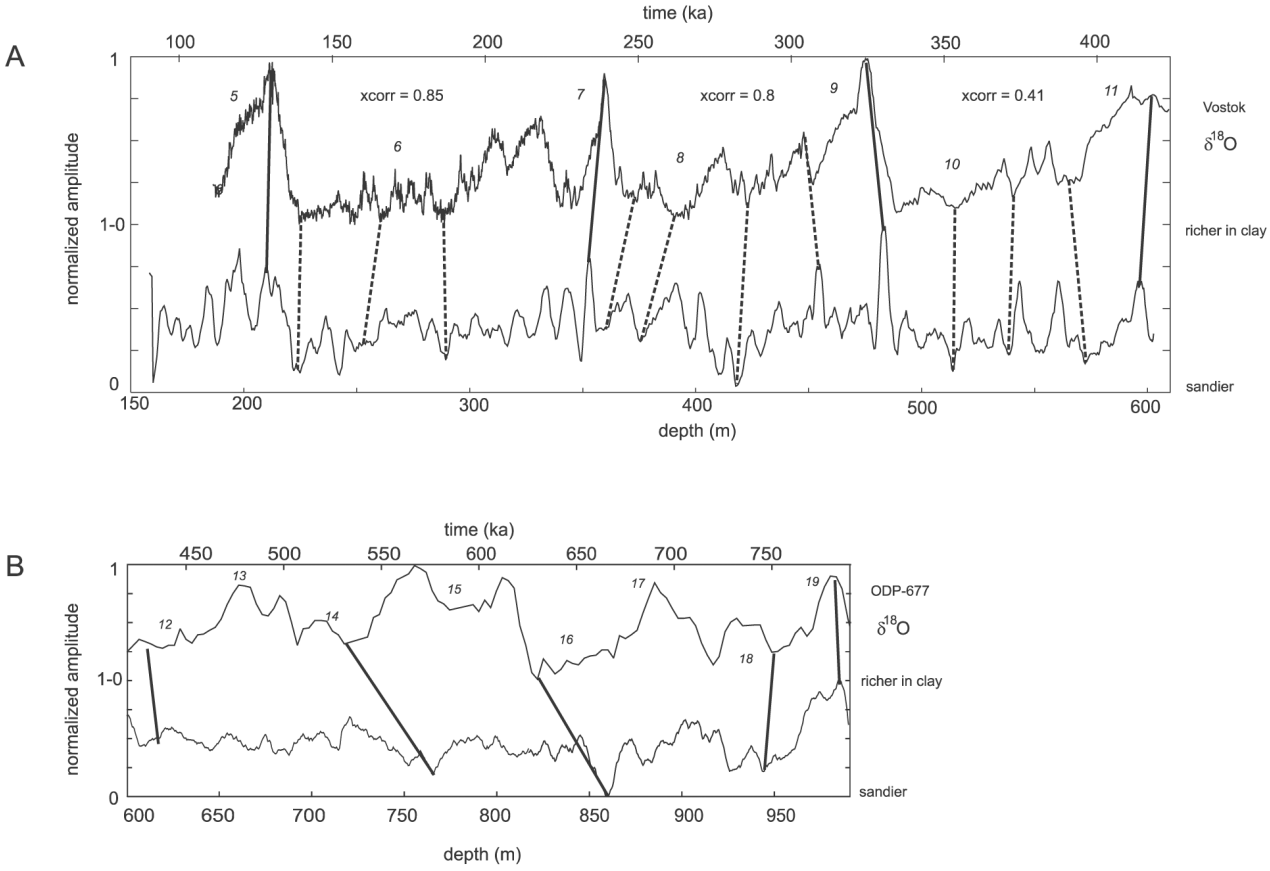


Fig. 3. Correlation between the ELS1 gamma-ray log and $\delta^{18}O$ signal from Vostok ice cores (A) and $\delta^{18}O$ from ODP 677 site (B). Vertical scale of both signals has been normalized. Gamma-ray log has been smoothed with a running average of 5 data points (1.2 m) for (A) and 9 data points (2 m) for (B).

case of the oxygen stage 11 at 410 ka, the stage at which we switch time scales, maxima of the Vostok ice cores and ODP 677 site differ about 10 kyr. The second effect arises from the fact that interstadial climatic changes -on millenial timescales- in opposite hemispheres are out of phase by about 1500 yr (Blunier *et al*., 1998), however the lack of that type of resolution in our present records minimizes this effect in our correlations. Finally, the different resolution of $\delta^{18}O$ curves accounts for uncertainties of a few thousand years or less, the largest being associated with ODP 677, which has a 3 kyr sampling interval.

To test how robust the correlation is, ages of tie-points were compared against two time-depth models (Figure 4): a linear model and an exponential model accounting for compaction. Note that the uncertainties discussed in the preced-

ing section are one half of the symbols used in the plots in Figure 4. The linear model is able to fit ages up to 400 ka, after that there is a significant departure (Figure 4), whereas the exponential model shows very low dispersion, fitting the tendency of the data.

Figure 4b illustrates a histogram of the residuals of the exponential model and it can be appreciated that it follows a Gaussian distribution with a standard deviation of ~9.7 kyr. What is important about this simple exercise is that the depth-age relation behaves as expected for a basin filled with clastic sediments as Laguna Salada is, *i.e.,* shallow sediments with little or no burden have ages that linearly increase with depth, and as lithostatic pressure increases compaction becomes an important effect. Moreover, dispersion in the data can be explained as stochastic processes associated with sedimentation or fault activity (Huybers, 2002).

**Tectonic implications**

Subsidence of rift basins in their initial stage is controlled by numerous seismic slip events localized along a set of collinear faults (*i.e.,* the bounding fault system) and by bending of the crust (King *et al*., 1989; Contreras *et al*., 1997; Cowie and Roberts, 2001); this gives rise to their characteristic half-graben geometry. Isostatic response to the filling of the depression created by faulting and flexure creates additional subsidence but this is a second order effect given the small density contrast between sediments and crust of ~10% (Contreras *et al*., 1997). Because of this, stratigraphy of rift basins relays information to constrain long-term subsidence rates and fault behavior (e.g., Cowie and Roberts, 2001; Contreras *et al*., 2000; Dawers and Underhill, 2000).

Drilling site ELS1 is located 5 km east of Laguna Salada fault, one of the faults controlling the subsidence of the Laguna Salada rift basin (Figure 1). Due to the proximity of the borehole to the bounding fault system we consider that sedimentation is a direct estimation of the subsidence induced by the Laguna Salada fault. The subsidence rate derived here is in agreement with independent measurements of the vertical slip rate of this fault, which we interpret as an indication of the validity of our assumption (see discussion below). However, damping from flexure might affect our estimate and it must be taken as a minimum of the rate of subsidence of this fault.

Our time series analysis suggests that subsidence rates within Laguna Salada remained constant during the deposition of the uppermost 980 m of sediments or, equivalently, during the last 780 ka, otherwise significant smearing would be observed in the gamma- ray log spectrum. Moreover, the close agreement between the ratio of the thickness of the sedimentary cicles and ratios of the Milankovitch cycles provide us with estimates of the subsidence rate, ranging from 1.36 mm/yr to 1.6 mm/yr with a mean value of 1.48 mm/yr. However, the exponential age-depth model hints that compaction should be accounted for and places the upper bound as a more realistic value (Figure 4).

The Laguna Salada-Cañada David fault system has been surveyed with different geophysical and geological methods, each giving different extension and/or vertical displacement rates. Savage *et al*. (1994), based on two geodesic transects 13 years apart crossing the Laguna Salada fault, obtained a horizontal extension rate of 4 mm/yr; Muller and Rockwell (1995) estimated a minimum vertical slip rate of 1.9±0.4 mm/yr for the same area based on inferred ages of paleosols; Dorsey and Martín-Barajas (1999) estimate 2-4 mm/yr of slip rate in the Cañón Rojo fault based on footwall uplift and Quaternary stratigraphy; Axen *et al*. (1999) found an extension rate of 2-4 mm/yr from deduced ages of fault scarps and their offsets at the Cañada David fault; Axen *et al*. (2000) also give a crude extension rate value of 1-1.6 mm/yr for Cañada David fault, this time based on thermal history modeling of plutonic rocks outcropping in Sierra El Mayor (Figure 1).

The subsidence rate obtained in this article was derived from data spanning 750 Ka and perhaps is one of the best resolved long-term rate of the northern gulf region. We believe that the subsidence rate at the ELS1 site contains uncertainties of a few tenths of a millimeter, assuming sedimentation has kept pace with subsidence during the last 780 kyr. Indeed this seems to be the case since the gamma-ray log does not show any thinning or thickening upward tendency.

This is also of relevance for the seismic hazard of the region. On February 23, 1892 the Laguna Salada fault ruptured generating an earthquake of estimated magnitude M 7-7.5 and a scarp on surface with a mean height of 6m (Muller and Rockwell, 1995). Our displacement rate estimate place the recurrence interval for such large events at ~1900 yr. Observe that this value is an upper bound since the drill site is 5 km away from the fault trace, therefore, the actual slip rate may be higher.

## CONCLUSIONS

A cross-spectral analysis of a gamma-ray log from a geothermal exploratory well drilled in Laguna Salada, northeast Baja California, with $\delta^{18}O$ climatic proxies reveals that this rift basin preserves a pristine record of past Quaternary climatic changes. What is new in paper is that we establish a correlation of the log with the high-resolution $\delta^{18}O$ climatic proxies to date sediments deposited in the basin with an estimated uncertainty ±10 kyr. This "climatic tuning" of the gamma ray log indicate that sedimentation rates at the drill-

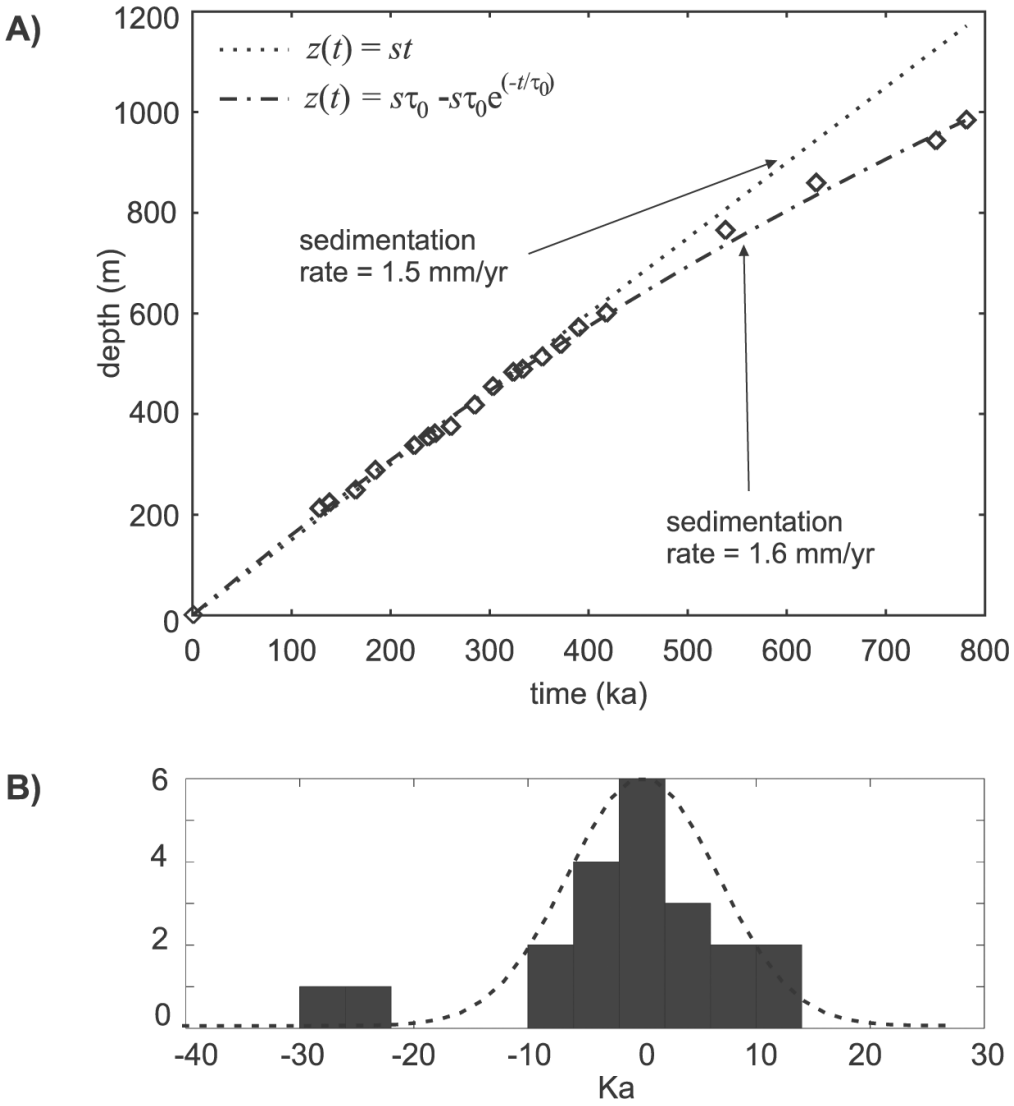


Fig. 4. (A) Time-depth conversion models for ELS1 site. Ages of tie-points in Figure 3 are shown as diamonds. The width of diamonds is twice the uncertainty of ages (~10 kyr) of tie points. Dotted line corresponds to the lineal model $z(t)=1.5$mm/yr $t$, whereas dashed line corresponds to the exponential model $z(t)=s\tau_0-s\tau_0 \exp(-t/\tau_0)$, where $s$=1.6 mm/yr and $\tau_0$=1530 kyr. (B) Histogram showing the distribution of the residuals of the exponential model and a Gaussian distribution model with a standard deviation of ~9.7 kyr.

ing site remained fairly constant at ~1.6 mm/yr during the last 780 ka. Given its proximity to the Laguna Salada fault we take this value as a direct estimation of the subsidence induced by this fault. This value is in agreement with independent estimations of the vertical slip rate of the Laguna Salada fault from other authors. However, it is likely that this value is damped by flexure and it should be taken as a minimum of the long-term subsidence rate of this fault.

## APPENDIX A: METHODOLOGY

In this section some basic elements of times series analysis are presented.

The autocorrelation function $R(t)$ of a continuous function $f(t)$ is defined by

$$R(t) = \int_{-\infty}^{\infty} f(t) f(t+\tau) d\tau .$$

The cross-correlation of two functions $f(t)$ and $g(t)$ of a real variable $t$ is defined by

$$f(t) * g(t) = \int_{-\infty}^{\infty} f(t)g(t-\tau)d\tau \, .$$

Now, the transformation $F(k)$ of a function $f(t)$ from the space or time domain $t$ to the frequency domain $k$ given by

$$F(k) = \int_{-\infty}^{\infty} f(t)e^{-2\pi ikt}dt \, ,$$

is called the forward Fourier transform and it carries a decomposition of the signal into sinusoidal waveforms of frequency $k$. The real function

$$H(k) = \left|F(k)\right|^2 ,$$

is the power spectrum of $f(t)$ and shows how power (energy per unit of time) is distributed among the waveforms of frequency $k$ constituting the signal $f(t)$. Finally, the coherence $C_{FG}(k)$ of two possibly related signals $f(t)$ and $g(t)$ with Fourier transforms $F(k)$ and $G(k)$, is given by

$$C_{FG}(k) = \frac{\left|F(k)G(k)\right|^2}{\left|F(k)\right|^2\left|G(k)\right|^2} \, .$$

A coherence value of 1 indicates signals at the frequency $k$ are a linear combination of each other, whereas a value of 0 indicates signals are uncorelated (e.g. g(t) is a noise process not derived from f(t)).

## ACKNOWLEDGEMENTS

We would thank the Mexican power company (CFE), especially Abril Gaspar, for providing the authors with copies of the gamma-ray log from ELS1 well and two anonymous reviewers for their helpful comments. Juan Contreras is grateful to Alejandro Nava and Alfonso Reyes for their valuable ideas and discussions on time series analysis and to José Mojarro for his computer expertise. Support from CICESE grant No 644107 (JC) and CONACyT grants 635229-T and U 42137-F (to JCH and JC) is acknowledged.

## BIBLIOGRAPHY

AXEN, G. J. and J. M. FLETCHER, 1999. Range-front fault scarps of the Sierra El Mayor, Baja California: formed above an active low-angle normal fault? *Geology, 27,* 247-250.

AXEN, G. J., M. GROVE, D. STOCKLY, O. M. LOVER, D. A. ROTHSTEIN, J. M. FLETCHER, K. FARLEY and L. ABBOT, 2000. Thermal evolution of Monte Blanco dome: low-angle normal faulting during Gulf of California rifting and late Eocene denudation of the eastern Peninsular Ranges. *Tectonics, 19, 2,* 197-212.

BLUNIER, T., J. CHAPPELLAZ, J. SCHWANDER, A. DÄLLENBACH, B. STAUFFER, T. F. STOCKER, D. RAYNAUD, J. JOUZEL, H. B. CLAUSEN, C. U. HAMMER and S. J. JOHNSEN, 1998. Asynchrony of Antarctic and Greenland climate change during the last glacial period. *Nature, 394,* 739-743.

CONTRERAS, J., C. H. SCHOLZ and J. C. P. KING, 1997. A model of rift basin evolution constrained by first-order stratigraphic observations. *J. Geophys. Res., 102, B4,* 7673-7690.

CONTRERAS, J., M. H. ANDERS and C. H. SCHOLZ, 2000. Growth of a normal fault system: Observations from the Lake Malawi Basin of the East African Rift system. *J. Struc. Geol., 97, 22,* 159-168.

COWIE, P. A. and G. P. ROBERTS, 2001. Constraining slip rates and spacings for active normal faults. *J. Struc. Geol., 23,* 1901-1915.

DORSEY, R. and A. MARTÍN-BARAJAS, 1999. Sedimentation and deformation in a Pliocene-Pleistocene transtensional supradetachment basin, Laguna Salada, north-west Mexico. *Basin Research, 11,* 205-221.

DAWERS, N. and R. UNDERHILL, 2000. The role of fault interaction and linkage in controlling synrift stratigraphic sequences: Late Jurassic, Statfjord east area, northern North Sea. *AAPG Bulletin, 84, 1,* 45-64.

HUYBERS, P., 2002. Depth and orbital tuning: a new chronology of glaciation and nonlinear orbital climate change. Ms. Sc. thesis, Massachusetts Institute of Technology, pp. 121.

IMBRIE, J. and J. Z. IMBRIE, 1980. Modeling the climatic response to orbital variations. *Science, 207,* 943-953.

KING, G. C. P., R. S. STEIN and J. B. RUNDLE, 1988. The growth of geological structures by repeated earthquakes. *J. Geophys. Res., 93,* 13307-13318.

MARTÍN-BARAJAS, A., S. VÁSQUEZ-HERNÁNDEZ, A. L. CARREÑO, J. HELENES, F. SUÁREZ-VIDAL and J. ALVARES-ROSALES, 2001. Late Neogene stratigraphy and tectonic control on facies evolution in the Laguna Salada Basin, northern Baja California, Mexico. *Sedimentary Geology, 144,* 5-35.

MULLER, K. J. and T. K. ROCKWELL, 1995. Late Quaternary structural evolution of the western margin of the Sierra Cucapá, northern Baja California. *Geol. Soc. Amer. Bull., 107,* 8-18.

OLSEN, P. E. and D. V. KENT, 1996. Milankovitch climate forcing in the tropics of Pangaea during the Late Triassic. *Palaeogeogr., Palaeoclim., Palaeoecol., 122,* 1 -26.

PETIT, J. R, J. JOUZEL, D. RAYNAUD, N. BARKOV, J. BANOLA, I. BASILE, M. BENDER, J. CHAPPELLAZ, M. DAVIS, G. DELAYGUE, M. DELMONTE, M. KOTLYAKOV, M. LEGRAND, V. LIPENKOV, C. LORIUS, L. PEPIN, C. RITZ, E. SALTZAMAN and M. STIVENARD, 1999. Climate and atmospheric history of the past 420,000 years from the Vostok ice core, Antarctica. *Nature, 399,* 429-436.

SAVAGE, J. C., M. LISOWSKI, N. E. KING and W. K. GROSS, 1994. Strain accumulation along the Laguna Salada fault, Baja California, Mexico. *J. Geophys. Res., 99,* 18109-18166.

SHACKLETON, N. J., A. BERGER and W. R. PELTIER, 1990. An alternative astronomical calibration of the lower Pleistocene timescale based on ODP 677. *Trans. R. Soc. Edinburgh, Earth Sciences, 81,* 251-261.

---

Juan Contreras[1], Arturo Martín-Barajas[2] and Juan Carlos Herguera[3]

*[1] Departamento de Geología, Centro de Investigación Científica y de Educación Superior de Ensenada (CICESE) Km 107 Carretera Tijuana-Ensenada, 22860 Ensenada B. C., México*
*Email: juanc@cicese.mx*
*[2] Departamento de Geología, Centro de Investigación Científica y de Educación Superior de Ensenada (CICESE) Km 107 Carretera Tijuana-Ensenada, Ensenada BC, 22860, México*
*Email: amartin@cicese.mx*
*[3] División de Oceanología, Centro de Investigación Científica y de Educación Superior de Ensenada (CICESE) Km 107 Carretera Tijuana-Ensenada, Ensenada BC, 22860, México*
*Email: herguera@cicese.mx*